Hindawi
Active and Passive Electronic Components
Volume 2019, Article ID 5716230, 5 pages
https://doi.org/10.1155/2019/5716230

Research Article

New Concept of Differential Effective Mobility in MOS Transistors

K. Bennamane and G. Ghibaudo

IMEP-LAHC, Minatec-INPG, 3 Parvis Louis Neel, BP 257, 38016 Grenoble, France

Correspondence should be addressed to G. Ghibaudo; ghibaudo@minatec.inpg.fr

Received 23 October 2018; Accepted 24 February 2019; Published 5 March 2019

Academic Editor: S. M. Rezaul Hasan

A new concept of differential effective mobility is proposed. It characterizes the effective mobility of an increment of drain current resulting from a small increase of inversion charge in MOSFET channel. It allows us to show that the effective mobility can be described by a local electric field approach and not entirely by an effective electric field model.

1. Introduction

The effective mobility μ_{eff} is one of the most important device parameters characterizing the transport in MOS transistors. The effective mobility in a MOSFET is intimately related to the average mobility of the carriers forming the inversion channel. From an experimental point of view, the effective mobility can be obtained by normalizing the drain current I_d in linear regime by the inversion charge Q_i as

$$\mu_{eff} = \frac{L}{W} \cdot \frac{I_d}{Q_i . V_d}. \quad (1)$$

where V_d is the drain voltage, L is the gate length, and W is the gate width. In general, the inversion charge is obtained by integration of the gate-to-channel capacitance $C_{gc}(V_g)$ in the so-called split C-V technique [1, 2].

In this work, we propose a new concept for the mobility, namely, the differential effective mobility, which characterizes the effective mobility of an increment of drain current resulting from a small increase of inversion charge.

2. Differential Mobility Concept

For a given DC bias, if the gate voltage of δV_g is increased, the drain current of δI_d will accordingly augment and the inversion charge of δQ_i. So, in analogy to (1), a differential effective mobility associated with the mobility of the small amount of carriers induced in the inversion layer by the gate voltage increase can be defined by

$$\mu_{diff} = \frac{L}{W} \cdot \frac{\delta I_d}{\delta Q_i . V_d}. \quad (2)$$

Therefore, (2) can be expressed in terms of transconductance, $g_m = \delta I_d/\delta V_g$, and gate-to-channel capacitance, $C_{gc} = \delta Q_i/\delta V_g$, as

$$\mu_{diff} = \frac{L}{W} \cdot \frac{g_m}{C_{gc} . V_d}. \quad (3)$$

It should be noted that μ_{diff} can be evaluated not only for the normal (or front) gate voltage but also for the back gate voltage V_b, i.e., the body bias for a bulk device, the substrate voltage for FD-SOI transistors, or the back gate voltage for double gate MOSFETs. In this case, in (3), g_m should be replaced by the body (or back gate) transconductance, $g_b = \delta I_d/\delta V_b$, and, C_{gc} by the body (or back gate)-to-channel capacitance, $C_{bc} = \delta Q_i/\delta V_b$.

In all the cases, given the definitions of g_m and C_{gc} (or C_{bc}), it is easy to show that the differential effective mobility μ_{diff} and the effective mobility μ_{eff} are related to each other as

$$\mu_{diff} = \mu_{eff} + Q_i \cdot \frac{\delta \mu_{eff}}{\delta Q_i}. \quad (4)$$

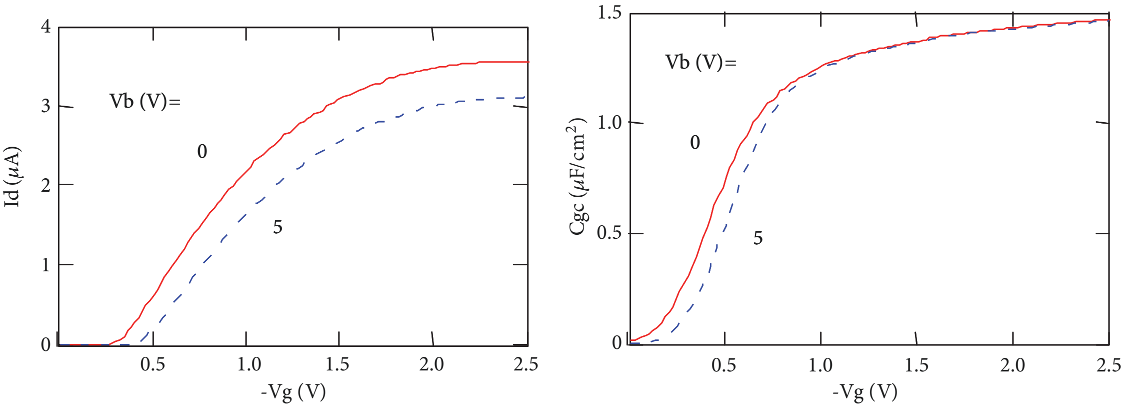

(a)

(b)

FIGURE 1: Typical $I_d(V_g)$ (a) and $C_{gc}(V_g)$ (b) characteristics obtained on p type FD-SOI MOSFETs for two substrate voltages V_b (W = 10 μm, L = 10 μm).

As will be shown below, it is interesting to discuss the notion of differential mobility in relation to the centroid of the inversion charge. Two charge centroids can similarly be defined [2]: (i) the DC centroid, X_{dc}, associated with the total inversion charge Q_i, and (ii) the AC centroid, X_{ac}, related to the incremental inversion charge δQ_i. In the case of a front gate modulation, X_{ac} can be obtained from the capacitance as [3, 4]

$$X_{ac} = \varepsilon_{si}\left(\frac{1}{C_{gc}} - \frac{1}{C_{ox}}\right). \tag{5}$$

where C_{ox} is the front gate oxide capacitance and ε_{si} the silicon permittivity.

X_{ac} and X_{dc} are related by the following differential equation [3]:

$$X_{ac} = X_{dc} + Q_i.\frac{\delta X_{dc}}{\delta Q_i}. \tag{6}$$

It can be shown by integration of (6) that X_{dc} can be calculated from X_{ac} as

$$X_{dc} = \frac{1}{Q_i - Q_{ith}} \int_{Q_{ith}}^{Q_i} X_{ac}(u)\, du \tag{7}$$

where Q_{ith} is a specific value of the inversion charge near threshold. One can show from simulation that X_{dc} and X_{ac} merge at threshold where (7) tends to the limit $X_{dc} = X_{ac}(Q_{ith})$.

3. Results and Discussion

$C_{gc}(V_g)$ and $I_d(V_g)$ measurements have been performed on FD-SOI and bulk devices. Here the μ_{diff} concept is illustrated with data taken on FD-SOI p type transistors, but similar results have been obtained on n and p type bulk structures. The FD-SOI devices feature a 2.2 nm gate oxide, a 145 nm bottom oxide, and an undoped silicon channel of thickness t_{si} = 10 nm.

Figure 1 shows typical $I_d(V_g)$ and $C_{gc}(V_g)$ characteristics for two substrate biases V_b. These curves have been used to calculate the corresponding $g_m(V_g)$, $g_b(V_g)$, and $Q_i(V_g)$ characteristics. The effective mobility and differential effective mobility have then been evaluated using (1) and (3). Their variations with inversion charge are shown in Figure 2(a), where μ_{diff} and μ_{diffb} refer to the font gate and back gate differential mobilities, respectively. As is usual μ_{eff} is found to be significantly attenuated at high inversion, mainly due to surface roughness (SR) scattering. Note that μ_{diff} is degrading faster than μ_{eff} with Q_i, whereas μ_{diffb} is slightly decreasing before reaching a plateau of higher value.

In order to better interpret these mobility data, we have extracted using (5)-(7) the variations with Q_i of the normalized centroids (X/t_{si}) of the total inversion charge, X_{dc}, and of incremental inversion charges for front gate and back gate modulation, X_{ac} and X_{acb} (see Figure 3(a)). As expected, X_{dc} and X_{ac} are getting closer to the front channel interface (zero on y-axis of Figure 3) as the transistor is pushed into stronger inversion [3, 4]. In contrast, the centroid of the incremental inversion charge induced by the back gate modulation, X_{acb}, is almost constant with Q_i and remains around the middle of the silicon film ($\approx 0.5\, t_{si}$). This allows us now to understand why μ_{diffb} was found nearly constant with Q_i and with a higher value. Indeed, μ_{diffb} refers to the effective mobility of carriers residing nearly in the middle of the film. In contrast, X_{ac} corresponds to carriers with a decreasing mobility as they are approaching the front interface, subjected to enhanced SR scattering.

Semiclassical TCAD simulations have been performed in such FD-SOI structures by considering two mobility approaches, i.e., either a local μ_{eff} model or a global one. In the local approach, μ_{eff} is a spatial function of the local electric field E_y like $\mu_{\text{eff}} = \mu_0/(1 + E_y/E_c)$ [5] and E_c is a critical field. In the global approach, μ_{eff} is calculated for the whole channel, using the effective electric field $E_{eff} = \int_0^{t_{si}} E_y(y)\, n(y)\, dy / \int_0^{t_{si}} n(y)\, dy$ (n being the carrier density) [6, 7], as $\mu_{\text{eff}} = \mu_0/(1 + E_{\text{eff}}/E_c)$. The simulation results shown in Figures 2(b) and 2(c) clearly indicate that only the

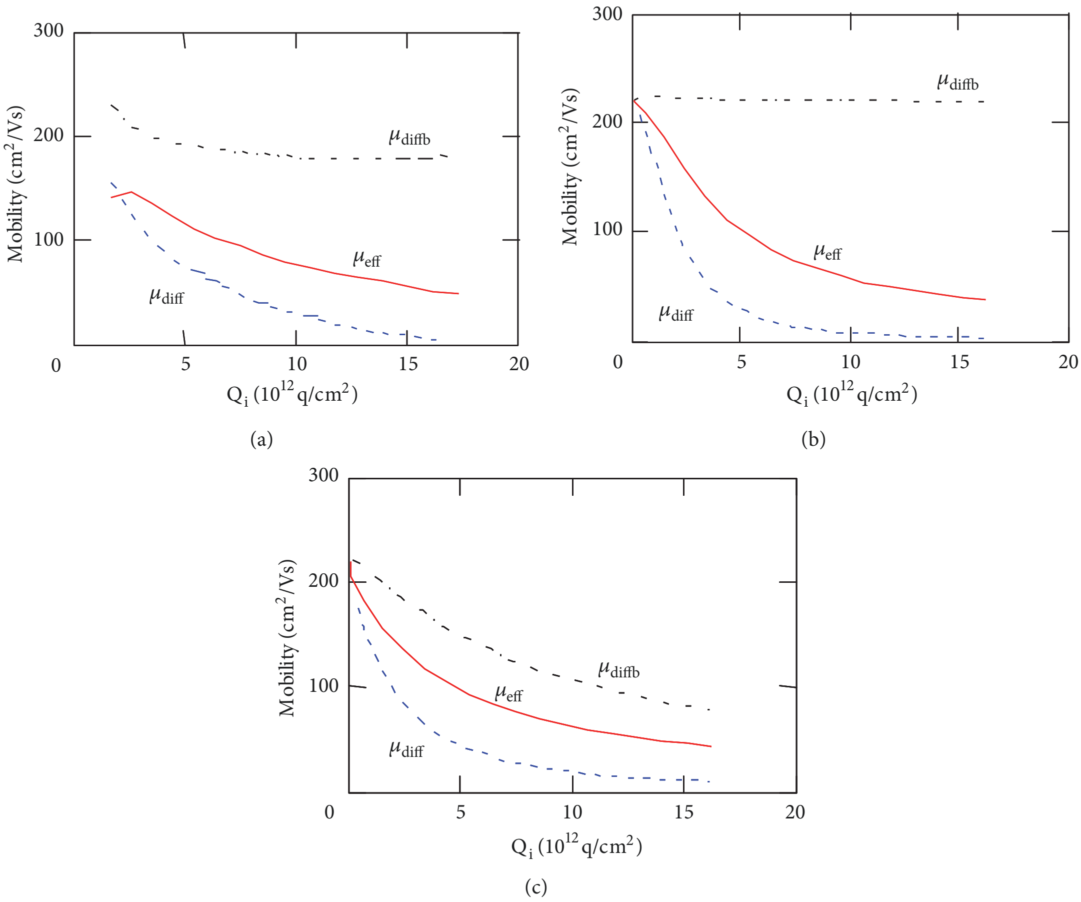

(a)

(b)

(c)

Figure 2: Variations of μ_{eff}, μ_{diff}, and μ_{diffb} with inversion charge Q_i as obtained from experiment (a) and from simulation in the local (b) or global (c) approaches (μ_0 = 220 cm^2/Vs, $E_c = 3 \times 10^5$ V/cm).

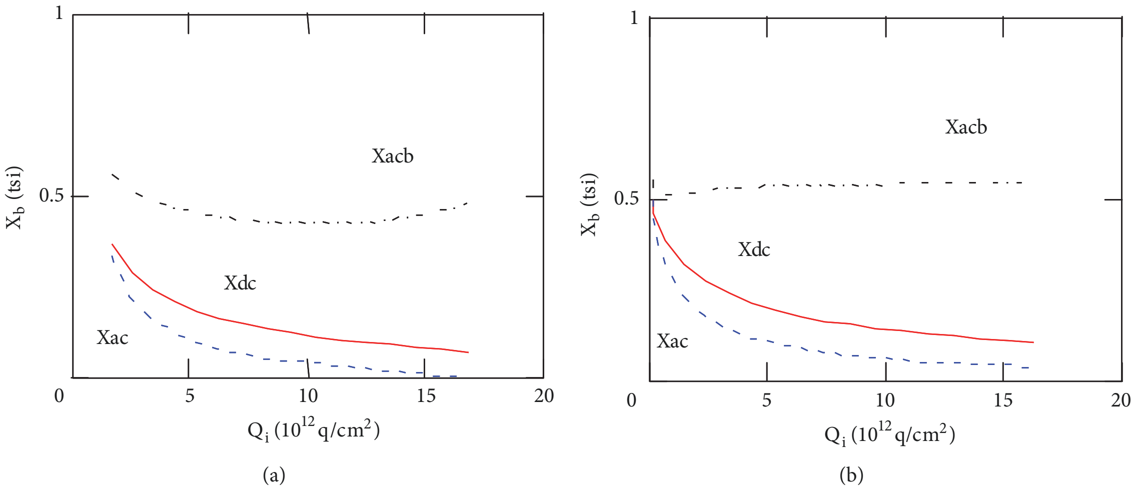

(a)

(b)

Figure 3: Variations of X_{dc}, X_{ac}, and X_{acb} with inversion charge Q_i as obtained from experiment (a) and simulation (b).

local mobility model provides an overall good description of the experimental mobility data (Figure 2(a)). Indeed, in the global approach, μ_{diffb} is strongly degraded at strong inversion due to the E_{eff} increase with V_g, whereas, in the local model, μ_{diffb} is almost constant, as in the experiment, since E_y cancels around midchannel. Note also from Figure 3 that the simulated variations of the centroids with Q_i well agree with the experimental ones, which emphasizes the analysis consistency. Finally, in Figure 4, in order to get a better physical insight, we have plotted the variations of the

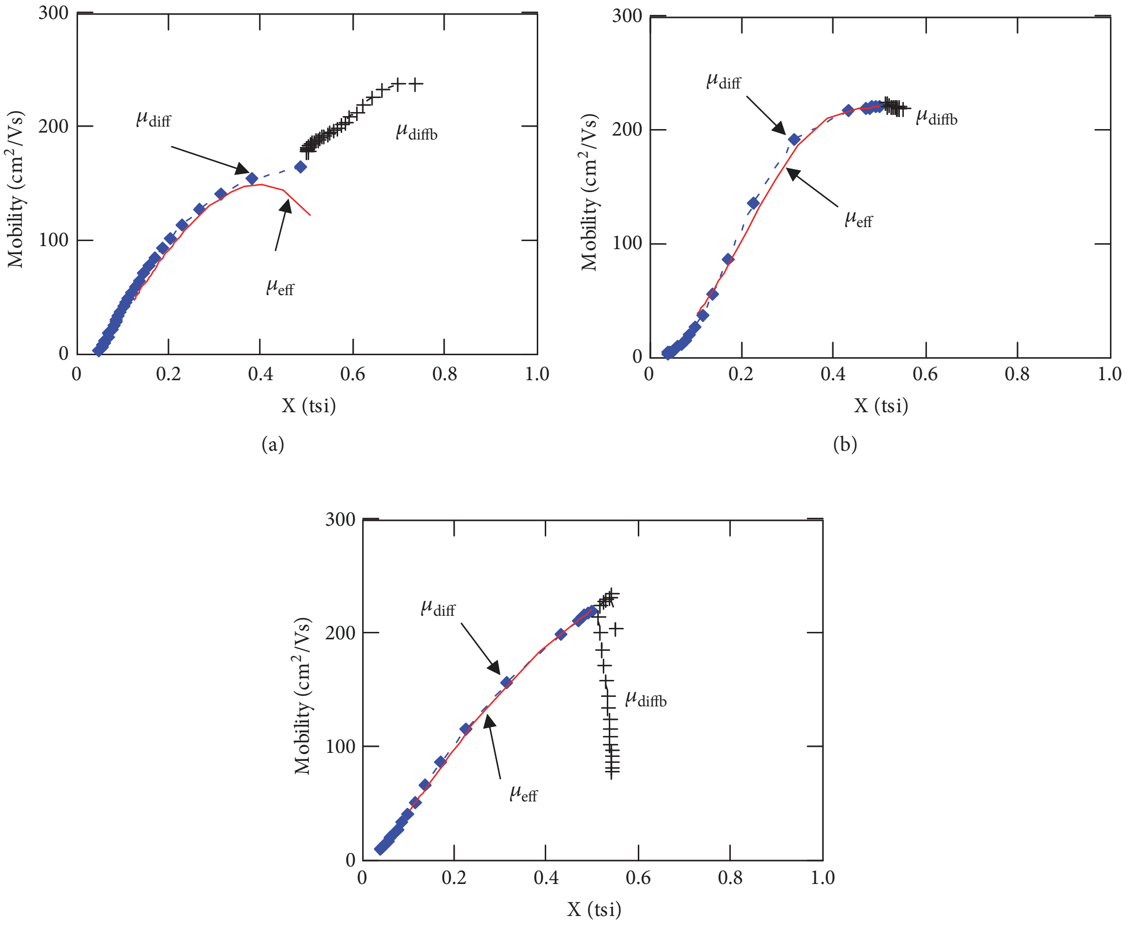

(a)

(b)

(c)

FIGURE 4: Variations of μ_{eff}, μ_{diff}, and μ_{diffb} with associated centroid X_{dc}, X_{ac}, and X_{acb} as obtained from experiment (a) and from local (b) and global (c) approaches.

various mobilities μ_{eff}, μ_{diff}, and μ_{diffb} as a function of their associated centroids X_{dc}, X_{ac}, and X_{acb}. Several features are worth noticing from these plots: (i) $\mu_{\text{eff}}(X_{dc})$ and $\mu_{\text{diff}}(X_{ac})$ nearly fall on the same graph, (ii) $\mu_{\text{diffb}}(X_{acb})$ prolongates the $\mu_{\text{diff}}(X_{ac})$ trends to smaller centroid values, and (iii) regarding simulation results, only the local mobility model provides again the good trend.

4. Conclusions

The concept of differential effective mobility has been demonstrated for the first time. It allowed us to show that the effective mobility can be described by a local electric field approach rather than an effective electric field one. This means that one cannot fully model the carrier mobility in MOSFET without a local model, especially in TCAD simulation. However, the existence of a $\mu_{\text{eff}}(E_{\text{eff}})$ universal curve and its use for experimental data analysis might remain more simple and appropriate for transport near the interface in single gate operation mode.

Data Availability

Figure's data used to support the findings of this study are available from the corresponding author upon request.

Conflicts of Interest

The authors declare that there are no conflicts of interest regarding the publication of this paper.

Acknowledgments

This work was performed with the support of author's employers, i.e., CNRS, for G. Ghibaudo and Univ. of Tizi-Ouzou for K. Bennamane.

References

[1] J. Koomen, "Investigation of the MOST channel conductance in weak inversion," *Solid-State Electronics*, vol. 16, no. 7, pp. 801–810, 1973.

[2] C. G. Sodini, T. W. Ekstedt, and J. L. Moll, "Charge accumulation and mobility in thin dielectric MOS transistors," *Solid-State Electronics*, vol. 25, no. 9, pp. 833–841, 1982.

[3] B. Yu, K. Imai, and C. Hu, "Electrical characterization of inversion layer carrier profile in deep-submicron p-MOSFETs," *Semiconductor Science and Technology*, vol. 12, no. 11, pp. 1355–1357, 1997.

[4] Y. Ma, Z. Li, L. Liu, and Z. Yu, "Comprehensive analytical physical model of quantized inversion layer in MOS structure," *Solid-State Electronics*, vol. 45, no. 2, pp. 267–273, 2001.

[5] M. N. Darwish, J. L. Lentz, M. R. Pinto, P. M. Zeitzoff, T. J. Krutsick, and H. H. Vuong, "An improved electron and hole mobility model for general purpose device simulation," *IEEE Transactions on Electron Devices*, vol. 44, no. 9, pp. 1529–1538, 1997.

[6] A. G. Sabnis and J. T. Clemens, "Characterization of the electron mobility in the inversion <100> Si surface," in *Proceedings of the International Electron Devices Meeting. IEDM Technical Digest*, pp. 18–21, Washington, DC, USA, 1979.

[7] S.-I. Takagi, A. Toriumi, M. Iwase, and H. Tango, "On the universality of inversion layer mobility in Si MOSFET's: part I—effects of substrate impurity concentration," *IEEE Transactions on Electron Devices*, vol. 41, no. 12, pp. 2357–2362, 1994.